Received: 2 February 2016 | Revised: 5 March 2016 | Accepted: 12 March 2016

DOI: 10.37917/ijeee.12.1.3 | Vol. 12| Issue 1 | June 2016

Open Access

Iraqi Journal for Electrical and Electronic Engineering

Original Article

Elliptical Annular Slot Loaded Trapezoidal Dipole Antenna for Band-Notched UWB Applications

Sarthak Singhal
Department of Electronics Engineering, IIT(BHU), Varanasi, UP, India-221005
ssinghal.rs.ece@iitbhu.ac.in

Nand Kishor Verma
Department of Electronics Engineering, IIT(BHU), Varanasi, UP, India-221005
nandkishorhbti@gmail.com

Amit Kumar Singh
Department of Electronics Engineering, IIT(BHU), Varanasi, UP, India-221005
aksingh.ece@iitbhu.ac.in

Abstract *In this paper, a semi-elliptical annular slot loaded trapezoidal dipole antenna with band-notched characteristics for UWB applications is designed. A microstrip feedline consisting of multiple feedline sections is used for improving the impedance matching. The band-notched characteristics for WLAN band are achieved by loading the trapezoidal dipole arms with semi-elliptical annular slots. The designed antenna structure has an operating range from 3.5-12.4 GHz(109%) with band-rejection in the frequency range of 5-6 GHz. Nearly omnidirectional patterns are achieved for the designed antenna structure. The designed antenna structure provided an average peak gain of 2.12 dB over the entire frequency range except in the notched band where it reduced to -2.4 dB. The experimental and simulation results are observed to be in good agreement. An improved bandwidth performance with miniaturized dimensions as compared to earlier reported antenna structures is achieved.*

***Index Terms*— Dipole antenna, elliptical annular slot, stepped feedline, trapezoidal patch, Ultrawideband (UWB) applications**

I. Introduction

In 2002, Federal Communication Commission (FCC) [1] allocated the unlicensed frequency spectrum from 3.1-10.6 GHz for ultra wideband technology. This allocation attracted several researchers both from academia and industry to utilize UWB technology in wireless communication devices. Several antenna structures [2-11] are investigated for the same purpose. The UWB signals got interference from commercially used WLAN (5-6 GHz) signals. To resolve this interference problem, various techniques like loading of the radiating patch with rectangular slots [2], T-shaped slots [3], U-slots [4] etc. In other configurations, ground plane was loaded with inverted L-shaped slots [10] etc.

In this paper, an elliptical slot loaded trapezoidal dipole antenna for UWB applications having band rejection function for the WLAN frequency band. is presented. The band rejection function for WLAN band is introduced into a trapezoidal dipole antenna by etching two semi-elliptical annular slots on each dipole arm. All the simulations are carried out using FEM based HFSS simulator software[12]. The impedance bandwidth is enhanced by using stepped feedline. The radiating patch of the designed antenna structure are trapezoidal in structure. The HFSS simulation results are verified by using FIT based CST MWS[13] simulator.

II. Antenna Design

The optimized geometry of the designed antenna structure is shown in Figure 1. The substrate used for designing the designed antenna structure is 1.6 mm thick FR-4 epoxy substrate having dielectric constant of 4.4, loss tangent of 0.02 and dimensions of L×W. The optimized dimensions of the designed antenna structure are listed in Table 1. The designed antenna structure is fed by a stepped microstrip feedline. The stepped feedline is designed by the combination of four feedline sections having different length and width. Due to the stepped structure of feedline, there is a smooth matching between the input impedance of dipole antenna and the impedance of coaxial probe.

Initially the double-printed trapezoidal patch dipole antenna (DPTPDA) [3] antenna structure dimensions are optimized on FR-4 epoxy substrate by the use of HFSS simulation software to achieve the UWB performance. The

optimization of various parameters of the designed antenna is done sequentially. During the optimization, the value of one dimension/parameter is varied by keeping the value of other dimensions/parameters fixed. The best variable parametric value is taken and other parameter is varied. This procedure is carried out repeatedly until the best reflection coefficient performance is achieved for final antenna design. After the optimization of DPTPDA dimensions, each dipole arm is loaded with semi-elliptical annular slit to achieve a band-notch characteristic in the frequency band of 5.125-5.825 GHz. The semi-elliptical annular slit is designed by using two concentric elliptical structures. Due to the etching of semi-elliptical slit on each dipole arm, the inner semi-elliptical section seems to be gap-coupled to the radiating patch.

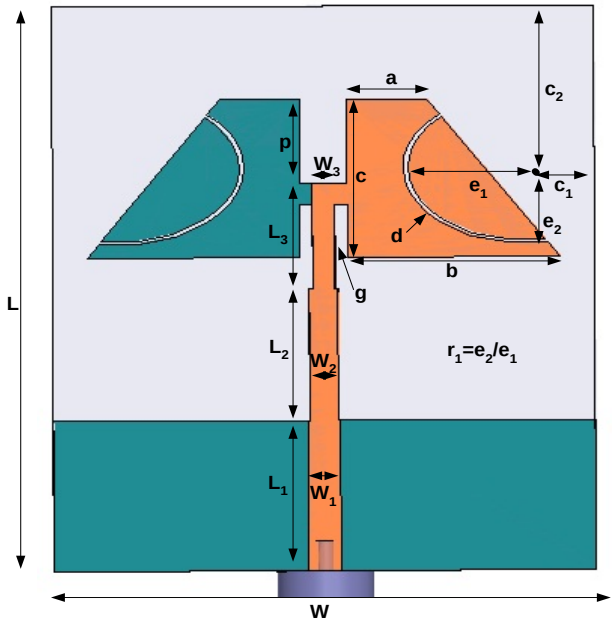

Figure 1 Configuration of the designed antenna

Table 1 Optimized dimensions of the designed antenna structure

Parameter	Value	Parameter	Value
L	37.5 mm	b	13.4 mm
L_1	10 mm	c	10 mm
L_2	8.7 mm	g	0.8 mm
L_3	7 mm	p	5.6 mm
W	34 mm	c_1	8.0 mm
W_1	2 mm	c_2	12.75 mm
W_2	1.8 mm	e_1	7.75 mm
W_3	1.4 mm	r_1	0.60 mm
a	5 mm	d	0.3 mm

III. Results And Discussion

To verify the HFSS simulation results for the designed antenna structure, CST MWS simulation software is used to simulate the antenna structure for the second time. After the validation of HFSS results by CST results, the prototype of the designed antenna structure, shown in Figure 2, is fabricated. The experimental measurement of the designed antenna structure is done using Agilent E8364B VNA. The comparison of reflection coefficient variation with respect to frequency obtained through HFSS & CST simulations and experimental measurement are shown in Figure 3 and listed in Table 2. A conclusion obtained after observing Figure 3 and Table 2 is that the experimental and simulation results have a good agreement. The mismatch observed in comparison between the measured and simulated results may be attributed to the fabrication errors or scattering environment during the measurement. The comparison among the VSWR plots of designed antenna structure with and without notch function is illustrated in Figure 4. It indicates that the incorporation of band notch function does not affect the antenna bandwidth.

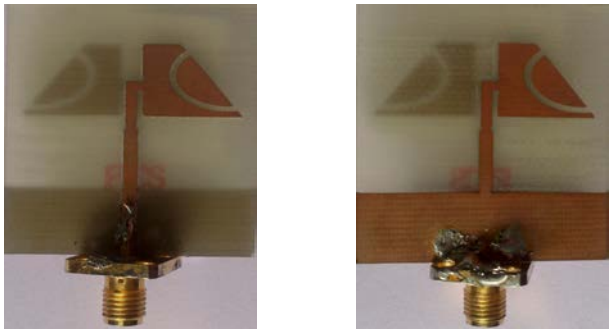

(a) Top View (b) Bottom View

Figure 2 Prototype of the designed antenna structure

Table 2 Tabular comparison of the measured and simulated results for the designed antenna structure

Software	Lower cut off frequency, f_L	Upper cut off frequency, f_H	Bandwidth, f_H-f_L	Notched Band
HFSS	3.67 GHz	12.3 GHz	8.63 GHz	4.7 GHz-5.8 GHz
CST	3.7 GHz	12.3 GHz	8.6 GHz	4.7 GHz-5.85 GHz
Measured	3.52 GHz	12.4 GHz	8.88 GHz	5 GHz-6.0 GHz

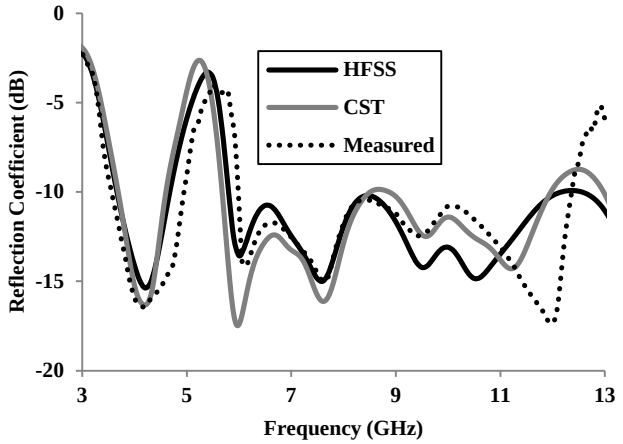

Figure 3 Comparison between the measured and simulated reflection coefficient versus frequency plots for designed antenna structure

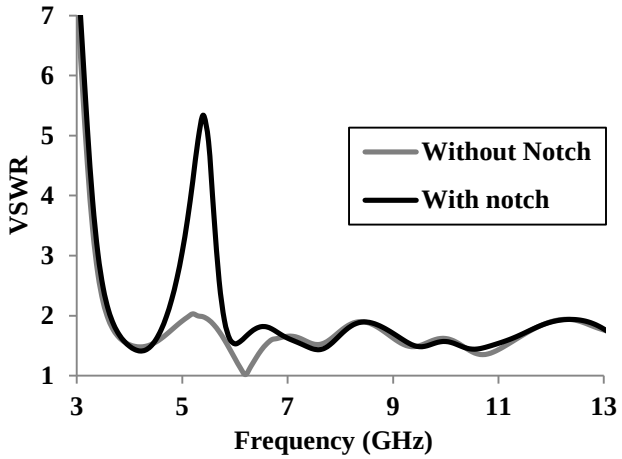

Figure 4 Comparison between the VSWR versus frequency plots for designed antenna structure with and without notch function

A comparison between the performance along with dimensions of the designed antenna structure and that of other dipole antenna structures available in the literature is shown in Table 3. Table 3 leads to an observation that the designed antenna structure has better performance in terms of impedance bandwidth and band-rejection characteristics along with an advantage of smaller size as compared to other antenna structures.

Table 3 Comparison of the designed antenna structure with other dipole structures already reported in the literature

Antenna	Size	Bandwidth	Band Notched	E-Plane Pattern	H-Plane Pattern	Gain (dB)
[2]	32x 30.3	3.15-12.03 GHz	5-6 GHz	Bi-directional, distorted at freq>10 GHz	Omnidirectional, distorted at freq>10 GHz	1-5 dBi
[3]	48× 46 mm^2	3-11 GHz	4.9-6.3 GHz	Bi-directional, distorted at freq>10 GHz	Omnidirectional, distorted at freq>10 GHz	3.6-5.9 dBi
[4]	91.7 x57	3-11 GHz	5.28 - 5.99 GHz	Directional	Directional	4-9 dBi
[5]	36× 36 mm^2	3-11 GHz	N.A.	Omnidirectional, distorted at higher frequency	Bi-directional, distorted at higher frequencies	1-5.5 dB
[6]	46× 48 mm^2	3-12 GHz	N.A.	Not given	Not given	Not given
[7]	48× 46 mm^2	2.95-11.76 GHz	N.A.	Approximately omnidirectional	Approximately omnidirectional	4.78 - 7.89 dB
[8]	71× 86 mm^2	3-11 GHz	N.A.	Distorted omnidirectional	Distorted omnidirectional	Values are not given

[9]	55×55 mm^2	2.56-10.40 GHz	N.A.	Omnidirectional, distorted at higher frequency	Bi-directional, distorted at higher frequencies	Not given
[10]	53×49 mm^2	3.656-15.64 GHz	5.06-6.012 GHz	Distorted omnidirectional	Bidirectional	Max. gain of 6.046 dB
Designed Antenna	**37.5×34 mm^2**	**3.52-12.4 GHz**	**5.0-6.0 GHz**	**Bi-directional, distorted at freq>10 GHz**	**Omnidirectional, distorted at freq>10 GHz**	**Average gain of 2.27 dB**

From the variation of real and imaginary parts of antenna input impedance with respect to frequency, shown in Figure 5, it is observed that the real part has its variation around 50 Ω and the imaginary part is oscillating around 0 Ω in the operating frequency band. Due to these variations the overall input impedance is approximately equal to 50 Ω i.e. the characteristic impedance of coaxial probe which results into better impedance matching.

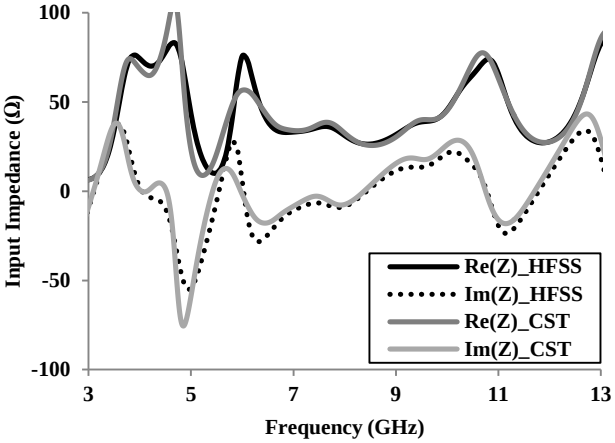

Figure 5 Variation of simulated real and imaginary parts of the input impedance of designed antenna structure

The measured radiation patterns of the designed antenna structure in two planes i.e. E-plane ($\Phi=0^o$) and H-Plane ($\Phi=90^o$) at its four resonance fr-equencies of 4.2 GHz, 6 GHz, 9.5 GHz and 10.5 GHz are shown in Figure 6. For the first resonance at 4.2 GHz, shown in Figure 6(a), the E-plane pattern is observed to have distorted dipole-shape whereas the H-plane pattern is found to be nearly omnidirectional. In case of second resonance frequency at 6 GHz, demonstrated in Figure 6(b), the nature of radiation patterns in both planes are observed to be similar to those at previous resonance. At the third resonance frequency of 9.5 GHz, shown in Figure 6(c), it is observed that both planes have quasi-omnidirectional radiation patterns. For the fourth resonance i.e. 10.5 GHz, depicted in Figure 6(d), it is found that the omnidirectional pattern is E-plane is not affected significantly but the H-plane pattern is very distorted.

The variation of measured peak gain with frequency for the designed antenna structure is demonstrated in Figure 7. From Figure 7, it can be seen that the peak gain has a maximum of 4.485 dB at the frequency of 11.2 GHz and a minimum of -0.6 dB at 3.5 GHz with an average of 2.12 dB in the entire frequency band. In the notched band, the peak gain value is -2.4 dB at 5.4 GHz. The peak gain performance is satisfactory as it shown a sharp reduction in the notched band.

The variation of total and radiation efficiencies of the designed antenna structure with frequency are shown in Figure 8. From Figure 8, it is observed that the radiation efficiency is more than 70 % and total efficiency is more than 65 % for the operating band. In the frequency range of 5-6 GHz i.e. notched band, the radiation efficiency decreased to 45 % whereas the total efficiency reduced to 25%.

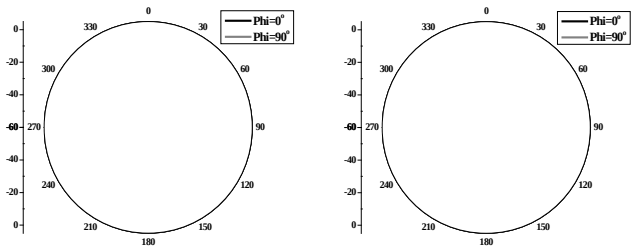

(a) 4.2 GHz (b) 6 GHz

The radiation patterns

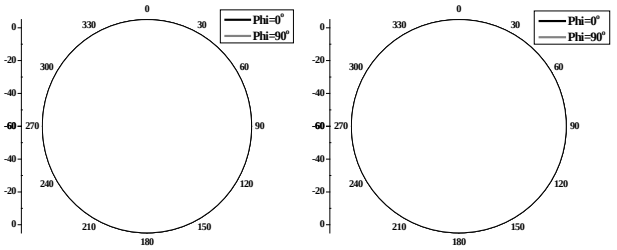

(c) 9.5 GHz (d) 10.5 GHz

The radiation patterns

Figure 6 Measured radiation patterns of the designed antenna structure at its resonance frequencies

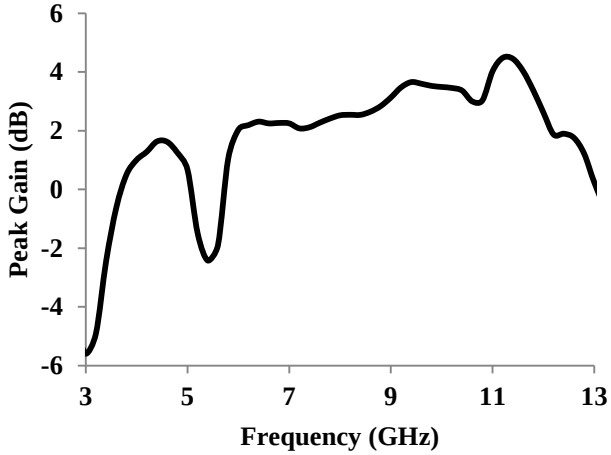

Figure 7 Measured peak gain versus frequency plot for the designed antenna structure

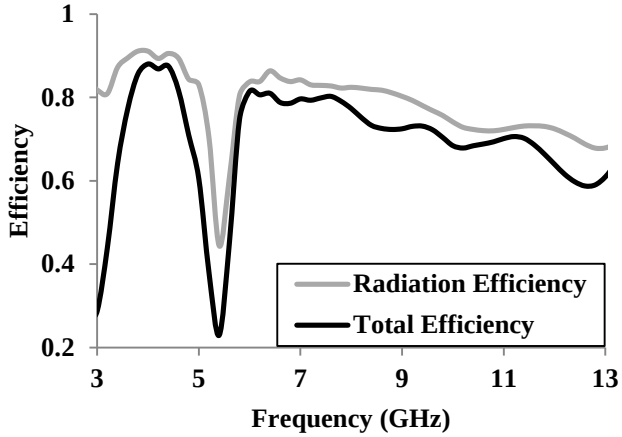

Figure 8 Total and radiation efficiency of the designed antenna structure

The pulse handling capability of the designed antenna structure is investigated by carrying out its time-domain analysis by using CST MWS simulation software. During the time domain analysis of the designed antenna structure, two configurations i.e. face to face and side by side, shown in Figure 9, are analyzed. In each configuration, two identical antenna structures are kept at a fixed distance of 30 cm. A Gaussian impulse is used for transmission and reception by each antenna structure. The normalized values of both transmitted and received pulses for both configurations are shown in. The correlation between the normalized transmitted and received pulses for both configurations, shown in Figure 10, are calculated by using a well defined parameter, fidelity factor [11] given by

$$F = \max\left[\frac{\int_{-\infty}^{\infty} s_r(t)s_t(t+\tau)d\tau}{\int_{-\infty}^{\infty}|s_r(t)|^2 dt \int_{-\infty}^{\infty}|s_t(t)|^2 dt}\right]$$

where, $s_r(t)$ and $s_t(t)$ are transmitted and received pulses respectively. The calculated values of fidelity factor in both configurations are shown in Table 4. From Table 4, it can be seen that in both configurations the correlation between the transmitted and received pulse is less. This less value of correlation indicates that the exciting signal is getting very much distorted by the designed antenna structure. It also indicates that the designed antenna structure has acceptable pulse handling capability suitable for UWB communication systems.

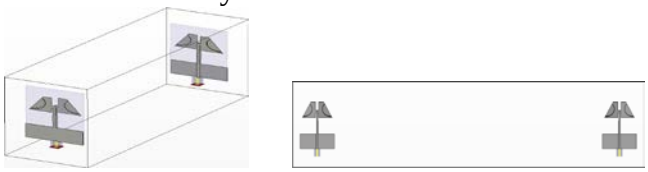

(a) Face To Face (b) Side By Side

Figure 9 Two configurations of the designed antenna for its time domain analysis

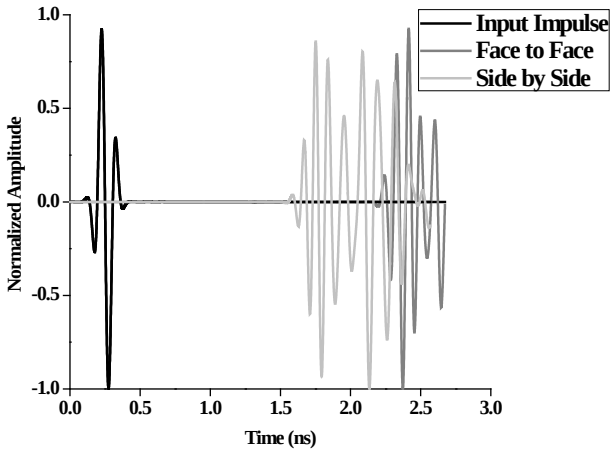

Figure 10 Simulated normalized transmitted and received impulses in two configurations

Table 4 Simulated Fidelity factor of the designed antenna structure in two configurations

Configuration	Face to face	Side by Side
Fidelity Factor	67	57

From the simulated group delay of the designed antenna structure, shown in Figure 11, it is observed that the group delay is varying between 0 ns to 1 ns over the entire frequency range. This value of group delay is within the desired limits for UWB communication.

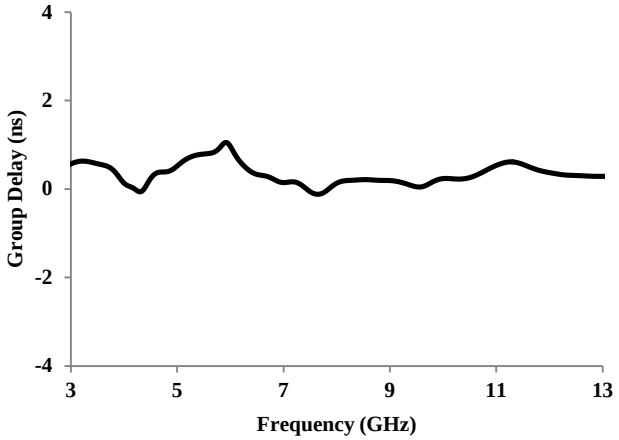

Figure 11 Simulated group delay of the designed antenna structure in face to face configuration

The magnitude of simulated transmission loss, $|S_{21}|$, versus frequency plots for both configurations are shown in Figure 12. From Figure 12, it is observed that both curves are varying between -50 dB to -75 dB in the frequency range of 3.5-8 GHz and -45 to -65 dB for the frequency range of 8-12.5 GHz. The simulated variation of phase of S_{21} for face to face configuration is shown in Figure 13. From Figure 13, it is observed that linear phase variations are achieved over the entire frequency range i.e. which ensures good pulse transmission capability.

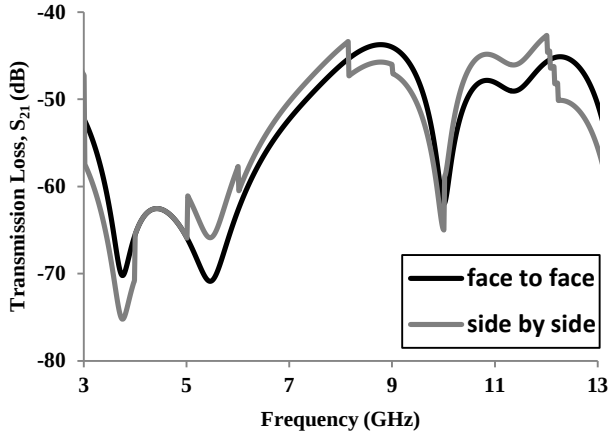

Figure 12 Simulated magnitude of transmission loss for the face to face configuration of the designed antenna structure

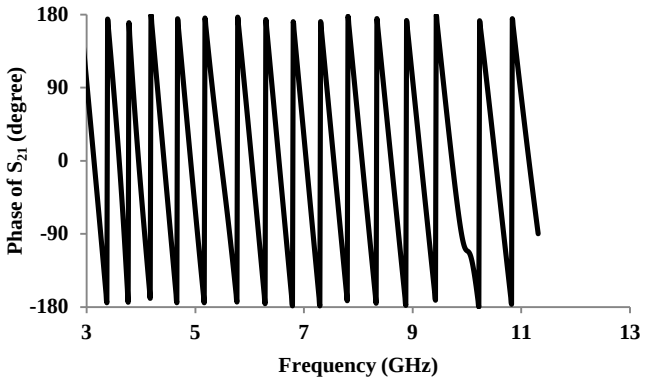

Figure 13 Simulated phase of transmission loss for face to face configuration of the designed antenna structure

IV. CONCLUSION

An elliptical annular slot loaded band-notched trapezoidal dipole antenna for UWB applications is designed and analyzed. The band-notch characteristics for WLAN frequency band i.e. 5-6 GHz is achieved by etching elliptical annular slots on the trapezoidal radiating arms. A

good agreement between the simulation and experimental results is found. The suitability of the designed antenna structure for UWB applications without interference from WLAN band is proved by the experimental results. It will find its application in the areas of Defence systems, radar and navigation systems, UWB, radiodetermination applications (4.5-7 GHz), WAS/RLANS (5.15-5.35 and 5.470-5.725 GHz), weather radars, ISM (5.725-5.875 GHz), RTTT (5.795-5.805 GHz and 5.805-5.815 GHz), Amateur Satellite (S/E) (5.830-5.850 GHz), ITS (5.875-5.925 GHz and 5.855-5.875 GHz), FSS, Mobile satellite applications (7.250-7.375 GHz), mobile applications (8.025-8.2 GHz) etc. [14]

ACKNOWLEDGMENT

Sarthak Singhal and Nand Kishor Verma are very thankful to the Ministry of Human Resource Development, Government of India, for providing the financial support in the form of teaching assistantship.

REFERENCES

[1] Federal Communication Commission, "First Order and Report: Revision of Part 15 of The Commission's Rules Regarding UWB Transmission Systems," April 22, 2002

[2] J. P. Zhang, Y. S. Xu, and W. D. Wang, "Microstrip-Fed Semi-Elliptical Dipole Antennas for Ultrawideband Communications," IEEE Transactions on Antennas And Propagation, Vol. 56, No. 1, Pp. 241-244, January 2008

[3] Y. S. Hu, M. Li, G. P. Gao, J. S. Zhang, and M. K. Yang, "A Double-Printed Trapezoidal Patch Dipole Antenna For UWB Applications With Band-Notched Characteristic," Progress In Electromagnetics Research, PIER, Vol. 103, pp. 259-269, 2010

[4] C. Yu, W. Hong, L. Chiu, G. Zhai, C. Yu, W. Qin, and Z. Kuai, "Ultrawideband Printed Log-Periodic Dipole Antenna With Multiple Notched Bands," IEEE Transactions on Antennas and Propagation, Vol. 59, No. 3, pp. 725-732, March 2011

[5] T. Karacolak, and E. Topsakal, "A Double-Sided Rounded Bow-Tie Antenna (DSRBA) For UWB Communications," IEEE Antennas and Wireless Propagation Letters, Vol. 5, pp. 446-449, 2006

[6] J. S. Zhang, and F. J. Wang, "Study of A Double Printed UWB Dipole Antenna," Microwave and Optical Technology Letters, Vol. 50, No. 12, pp. 3179-3181, 2008

[7] G. P. Gao, X. X. Yang, J. S. Zhang, J. X. Xiao, and F. J. Wang, "Double-Printed Rectangular Patch Dipole Antenna For UWB Applications," Microwave and Optical Technology Letters, Vo. 50, No. 9, pp. 2450-2452, 2008

[8] T. G. Ma, and S. K. Jeng, "A Printed Dipole Antenna With Tapered Slot Feed for Ultra-Wideband Applications," IEEE Transactions on Antennas and Propagation, Vol. 53, No. 11, pp. 3833-3836, 2005

[9] J. P. Zhang, Y. S. Xu and W. D. Wang, "Ultra-Wideband Microstrip-Fed Planar Elliptical Dipole Antenna," Electronics Letters, No. 42, No. 3, 2006

[10] K. Shambavi, and Z. C. Alex, "Printed Dipole Antenna With Band Rejection Characteristics for UWB Applications," IEEE Antennas And Wireless Propagation Letters, Vol. 9, pp. 1029-1032, 2010

[11] S. Singhal, and A. K. Singh, "Crescent-Shaped Dipole Antenna For Ultrawideband Applications," Microwave and Optical Technology Letters, Vol. 57, No. 8, pp. 1773-1782 2015.

[12] HFSS, "High Frequency Structure Simulator ver. 11, Finite Element Package," Ansoft Corporation,
Available: http://www.ansoft.com, 2009.

[13] CST Microwave Studio Suite 2011, CST Inc., 2007

[14] Electronic Communications Committee (ECC), "The European table of Frequency Allocations and Applications," ERC Report 25, approved May 2014